

Tectonics of the Jurassic- Early Cretaceous magmatic arc of the north Chilean Coastal Cordillera (22°-26°S): A story of crustal deformation along a convergent plate boundary

Ekkehard Scheuber and Gabriel Gonzalez¹

Institut für Geologie, Geophysik und Geoinformatik, Freie Universität Berlin, Berlin

Abstract. The tectonic evolution of a continental magmatic arc that was active in the north Chilean Coastal Cordillera in Jurassic-Early Cretaceous times is described in order to show the relationship between arc deformation and plate convergence. During stage I (circa 195-155 Ma) a variety of structures formed at deep to shallow crustal levels, indicating sinistral arc-parallel strike-slip movements. From deep crustal levels a sequence of structures is described, starting with the formation of a broad belt of plutonic rocks which were sheared under granulite to amphibolite facies conditions (Bolfin Complex). The high-grade deformation was followed by the formation of two sets of conjugate greenschist facies shear zones showing strike-slip and thrust kinematics with a NW-SE directed maximum horizontal shortening, i.e., parallel to the probable Late Jurassic vector of plate convergence. A kinematic pattern compatible to this plate convergence is displayed by nonmetamorphic folds, thrusts, and high-angle normal faults which formed during the same time interval as the discrete shear zones. During stage II (160-150 Ma), strong arc-normal extension is revealed by brittle low-angle normal faults at shallow levels and some ductile normal faults and the intrusion of extended plutons at deeper levels. During stage III (155-147 Ma), two reversals in the stress regime took place indicated by two generations of dikes, an older one trending NE-SW and a younger one trending NW-SE. Sinistral strike-slip movements also prevailed during stage IV (until ~125 Ma) when the Atacama Fault Zone originated as a sinistral trench-linked strike-slip fault. The tectonic evolution of the magmatic arc is interpreted in terms of coupling and decoupling between the downgoing and overriding plates. The structures of stages I and IV suggest that stress transmission due to seismic coupling between the plates was probably responsible for these deformations. However, decoupling of the plates occurred possibly due to a decrease in convergence rate resulting in extension and the reversals of stages II and III.

1. Introduction

Active continental margins are sites of strong crustal deformations which are generally considered to be driven by plate conver-

gence [e.g., Jarrard, 1986]. However, besides this generally accepted dependence, the origin and the nature of the driving mechanisms for the deformations are still unclear. In literature, two possible sources are proposed for the stresses leading to deformations in the upper plate: (1) seismic coupling in the case of high-stress subduction zones [Uyeda and Kanamori, 1979; Miura *et al.*, 1989; Tichelaar and Ruff, 1993; Liu *et al.*, 1995] and (2) flow of asthenospheric material in the mantle wedge beneath the upper plate ("corner flow") [Andrews, 1972] for low-stress subduction zones [Uyeda and Kanamori, 1979].

In models invoking seismic coupling [Fitch, 1972; Uyeda and Kanamori, 1979; Geist and Scholl, 1992; Platt, 1993] the tectonic forces responsible for upper plate deformations are induced by the subducting plate that shears the overriding plate along the subduction zone and horizontally indents the overriding plate inland [Wdowinski and Bock, 1994]. On the other hand, Furukawa [1993a, b] has shown that asthenospheric corner flow induced by viscous drag above a subducting slab is able to produce differential stresses of the order of 100 MPa at the base of the upper plate's lithosphere and that the maximum stress is vertical beneath the arc and becomes horizontal toward the forearc. These stresses may exceed the frictional stresses in the seismogenic part of the plates' interface, which are only of the order of a few tens of megapascals [Peacock, 1992; Gephart, 1994; Wang *et al.*, 1995; Ponko and Peacock, 1995].

One possibility to test whether seismic coupling is responsible for the deformations in the upper plate's crust is to study the structures of the magmatic arc, because due to magmatic heating, this is the weakest part of the upper plate, which thus deforms very easily. Most of the structures forming in the arc are related to trench-parallel fault systems (TPFSs, trench-linked strike-slip faults in the sense of Woodcock [1986]), and the kinematic patterns in the arc and the displacements along the TPFS are indications of movements of the rigid forearc sliver relative to the upper plate. If these kinematic patterns are controlled by stresses related to seismic coupling, the general movement along the TPFS must be syntheical to the convergence vector (e.g., dextral oblique convergence should result in dextral displacements along the TPFS) [Fitch, 1972; Geist and Scholl, 1992; Platt, 1993]. On the other hand, if the kinematic patterns of the arc are antithetical to the convergence vector (e.g., dextral displacements in a system of sinistral plate convergence), seismic coupling can be ruled out as a driving mechanism for forearc movements; in this case other forms of stress transmission (e.g., corner flow) from the lower plate to the upper plate have to be taken into account. Thus, when reversals in the sense of displacement occur along the TPFS, changing conditions of coupling and decoupling between the plates can be inferred.

The central Andes, where subduction is an ongoing process since the Early Jurassic, are a very suitable area to investigate the relationship between upper plate tectonics and plate convergence,

¹Now at Departamento de Ciencias Geológicas, Universidad Católica del Norte, Antofagasta, Chile.

since subduction led to the formation of four magmatic arcs in all of which TPFSSs have developed. The most prominent faults are the Late Jurassic-Early Cretaceous Atacama Fault Zone [Arabasz, 1971; Scheuber and Andriessen, 1990; Brown *et al.*, 1993] in the Coastal Cordillera and the late Eocene Precordilleran Fault System in the north Chilean Precordillera from which a strike-slip reversal from dextral to sinistral displacements has been described by Reutter *et al.* [1996].

The aim of this paper is to draw conclusions from the tectonic evolution of the Jurassic-Early Cretaceous magmatic arc of northern Chile on the convergence history and the state of plate coupling during that time. In reconstructing the tectonic evolution of this arc we found that oblique shortening was a very important process, suggesting that arc deformations occurred because of oblique convergence. This idea is in agreement with paleogeodynamic reconstructions that previous workers have proposed (Figure 1) [Larson and Pitman, 1972; Zonenshayn *et al.*, 1984; Jaillard *et al.*, 1990].

2. Geology and Tectonics of the Coastal Cordillera

The tectonic evolution of the north Chilean central Andes is characterized by subduction-induced magmatism which has been active at least since 200 Ma (Andean Cycle) [Coira *et al.*, 1982]. Owing to an eastward migration of igneous activity since the Early Cretaceous, it is possible to distinguish four magmatic arcs [Scheuber and Reutter, 1992]: a Jurassic-Early Cretaceous arc (200-120 Ma) in the Coastal Cordillera, a mid-Cretaceous arc (110-75 Ma) in the Longitudinal Valley, a latest Cretaceous-Paleogene arc (72-34 Ma) in the Chilean Precordillera, and the late Oligocene-Holocene arc (25-0 Ma) in the Western Cordillera.

The Jurassic-Early Cretaceous magmatic arc (Figure 2) is composed of mantle-derived igneous rocks [Rogers and Hawkesworth, 1989] which make up ~80% of the crust of the Coastal Cordillera [Scheuber, 1994], whereas ensialic pre-An-

dean units (before 200 Ma) form only a minor fraction (<15%). Volcanism, which was active in Early to Middle Jurassic times (middle Sinemurian to upper Callovian) [Kossler, 1996], led to the deposition of a 5-10 km thick volcanic pile mainly composed of basaltic andesitic lavas and tuffs (La Negra Formation) [García, 1967]. Marine intercalations of Bajocian age within these volcanics indicate a deposition in a subsiding basin, and no high mountain range was formed. A lowland topography in the realm of the volcanic arc can also be inferred from the observation that the sediments of the marine backarc basin, bordering the arc to the east, received only little detritus from the arc. Thus, as the input of magmas into the crust was not associated with mountain building and crustal thickening, igneous activity must have been accompanied by strong crustal extension. Plutonism, which also started around 200 Ma [Boric *et al.*, 1990], led to the formation of numerous intrusive bodies of various shape and size with gabbroic to granodioritic composition, most of which intruded at shallow crustal levels [Dallmeyer *et al.*, 1996]. According to available isotope age data, plutonism had its maximum in Middle Jurassic to Early Cretaceous times (160-120 Ma) [Boric *et al.*, 1990], that is, the majority of plutons are coeval with or younger than the final stages of volcanism.

For the understanding of the kinematic pattern in a magmatic arc, the knowledge of plate kinematics is important. Off South America no oceanic crust older than some 50 Myr exists [Müller *et al.*, 1997]. Thus the only reconstructions of Mesozoic plate configurations in the Pacific realm are based on investigations of remnants of Jurassic and Cretaceous oceanic crust which still exist in the western Pacific [Larson and Pitman, 1972; Zonenshayn *et al.*, 1984]. These reconstructions (Figure 1) indicate that a SW-NE trending spreading center existed off South America, which Jaillard *et al.* [1990] interpreted as a southwestward continuation of the Thetys rift. However, besides these general reconstructions of the gross plate geometry, no data exist on important parameters such as convergence rate, slab dip, and age of the downgoing plate.

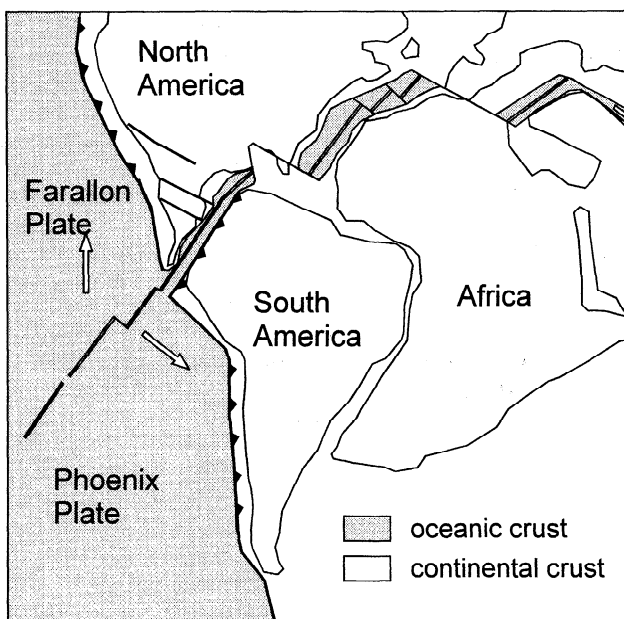


Figure 1. Paleogeodynamic reconstruction of the SE Pacific plate configuration during Jurassic and Early Cretaceous [modified after Jaillard *et al.*, 1990].

3. Structures of the Magmatic Arc

According to their relative age and kinematic pattern, the structures of the Jurassic-Early Cretaceous magmatic arc can be attributed to four stages which will be described in sections 3.1-3.4: (1) older arc-parallel sinistral movements, (2) crustal extension and magmatic growth of the arc, (3) oblique dilation due to the intrusion of dikes, and (4) younger arc-parallel sinistral movements.

3.1. Stage I: Older Sinistral Movements

3.1.1 Structures formed under high- to low-grade metamorphic conditions. High-grade shear zones, made up of amphibolites, orthogneisses, and sillimanite-andalusite-bearing paragneisses, have been described as "Jurassic shear zones" by Scheuber and Andriessen [1990] from north of Papos. In these arc-parallel shear zones the sense of shear is uniformly sinistral. However, sheared rocks of a deep crustal origin are most widespread south of Antofagasta and in the southern part of Mejillones Peninsula (Figure 2). Here the so-called "Bolfín Complex" [Rössling, 1989; Lucassen and Franz, 1994; González, 1996] is exposed, which forms a 20 km wide, N-S trending sheared belt consisting of foliated Jurassic quartz diorites to gabbros which south of Antofagasta show a nearly horizontal primary layering.

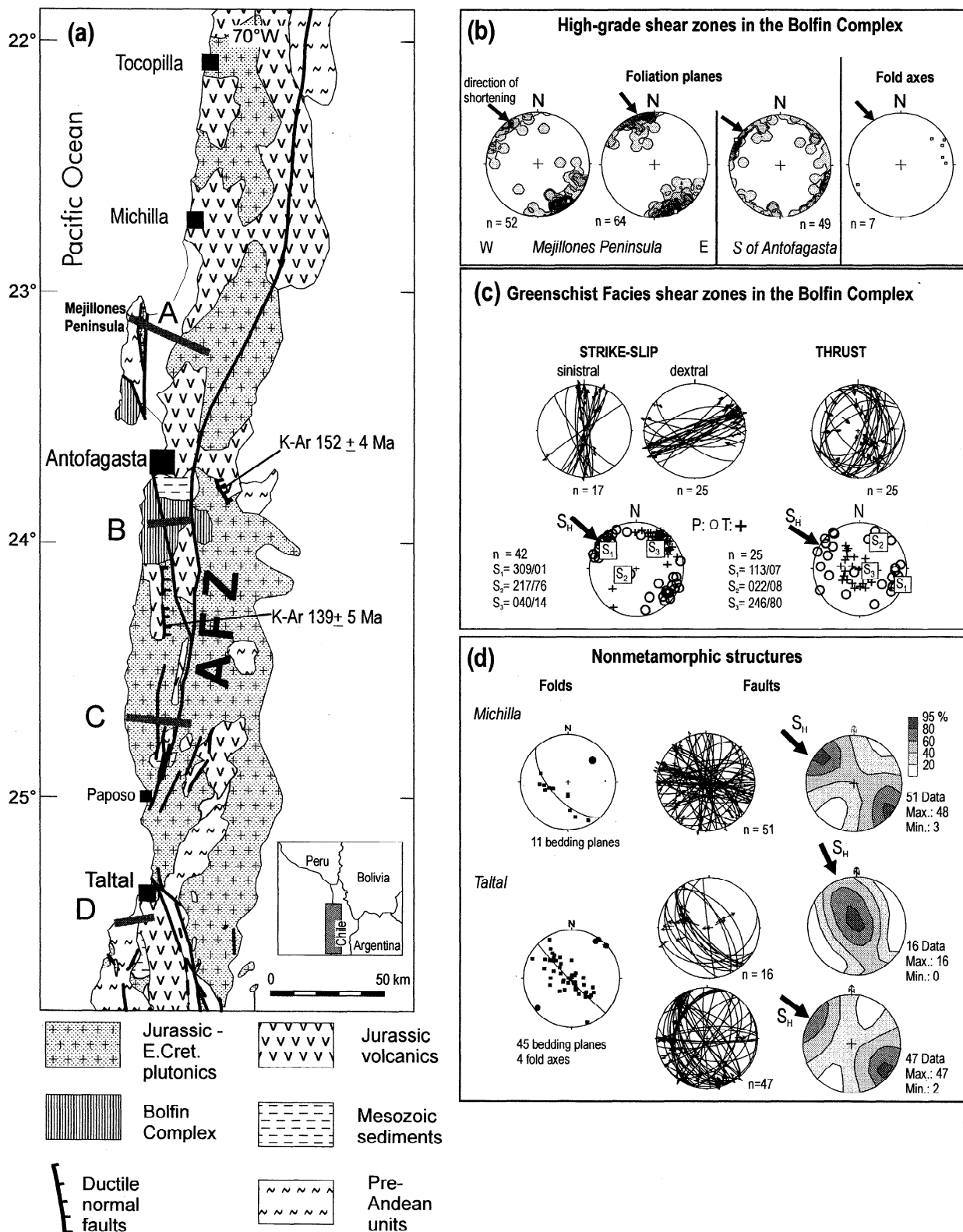


Figure 2. (a) Geological sketch map of the north Chilean Coastal Cordillera. Lines A-D refer to sections where dikes have been measured; locations of dated mylonite samples of ductile normal faults are also shown, AFZ, Atacama Fault Zone. (b) Pole figures (all diagrams are equal-area, lower hemisphere projections) of foliation planes of the fully ductile shear zones (density diagrams) and the orientations of fold axes (point diagram) from high-grade mylonites of the Bolfin Complex. (c, d) Orientations of strain directions of greenschist facies discrete shear zones and of nonmetamorphic structures. All structures have in common a NW-SE to NNW-SSE oriented direction of shortening and/or maximum horizontal stress S_H which match the NW-SE directed oblique plate convergence (see Figure 1).

Paleothermobarometric investigations (two-pyroxene and plagioclase-hornblende thermometry and hornblende barometry) [Lucassen and Franz, 1996; González, 1996] indicate that the intrusion and deformation of the Bolfin Complex rocks took place at pressures <500 MPa and at temperatures ranging from granulite to upper greenschist facies conditions (800–400°C). Deformation was strongly influenced by magmatic activity as, for example, foliated quartz-plagioclase veins and mafic dikes were sheared during the intrusion [Skarmeta, 1980] (Figure 3c). This is consistent with the findings of Brown *et al.* [1993], who reported granitic veins, lenses, and melt segregations oriented parallel to shear planes, which they interpreted as residual melts coeval to deformation.

The Bolfin Complex shows a variety of ductile to semiductile structures, all of which indicate NW-SE directed shortening due to N-S directed (arc parallel) sinistral strike-slip movements. These structures include: (1) fully ductile, high-grade shear zones, (2) numerous discrete, greenschist facies shear zones, and (3) folds.

3.1.1.1. High-grade shear zones: Most rocks of the Bolfin Complex are pervasively foliated amphibolitic gneisses and amphibolites showing dynamic recrystallization and later static recovery of all major constituents, plagioclase, amphiboles, orthopyroxene, and clinopyroxene. The lack of brittle porphyroclasts indicates that these rocks were deformed under fully ductile conditions. This corresponds to metamorphic conditions, which range from granulite to upper amphibolite facies at low pressure (600–800°C and <500 MPa) reported by Lucassen and Franz [1994, 1996] and González [1996].

The rocks of the Bolfin Complex display steep to vertical foliation planes which strike NE-SW in the western and central parts of the complex, whereas along the eastern margin the foliation is bent into a N-S direction. The rocks with NE-SW striking foliation are medium grained (grain size 5–10 mm) S-tectonites with low finite strain (R_{yz} between 1.5 and 4) [González, 1996] whereas the rocks from the eastern margin are highly strained S-L mylonites with a strongly reduced grain size of 0.20–0.25 mm and with well-developed stretching lineations plunging gently toward north (pitch ~35°). East of Antofagasta the high-strain mylonites are amphibolites which in parts have been migmatized by quartz-dioritic melts which intruded along foliation planes and which exhibit a magmatic flow fabric. These migmatized rocks give evidence that strongly foliated domains of the magmatic arc were sites of focused channeling of magma into the ductile crust. Various kinematic indicators, for example, subvertical folds with S geometries, reveal a sinistral sense of the shear in the mylonites.

3.1.1.2. Greenschist facies shear zones: The pervasively foliated rocks of the Bolfin Complex are cut by numerous discrete shear zones (1–2 m thick; Figure 3) which form two conjugate sets (Figure 2c): One set, showing strike-slip displacements, comprises vertical shear zones with horizontal stretching lineations, ENE-WSW trending dextral shear zones, and N-S trending sinistral shear zones. The other set consists of low-angle shear zones dipping toward SE and NW containing down dip stretching lineations and kinematic indicators revealing thrusting toward NW and SE. Field observations such as strike-slip shear zones grading laterally into thrust shear zones and vice versa suggest that both sets were formed simultaneously. The rocks of the conjugate shear zones are well-developed S-C mylonites indicative of semiductile deformation [Shimamoto, 1989]; this is corroborated by the observation that plagioclase, amphibole, and pyroxene form brittle porphyroclasts whereas biotite, actinolite, oligoclase, and quartz are recrystallized and/or newly crystallized, indicating upper greenschist facies conditions during deformation.

In the semiductile conjugate shear zones, shortening directions have been determined from the orientations of foliation planes and stretching lineations (Figure 2c). The method used was similar to that of paleostress reconstruction using brittle fault slip data [Angelier and Mechler, 1977; Angelier, 1984, 1994; Marret and Allmendinger, 1991]. We have measured the obtuse angle between the shear planes (C planes) of both the sinistral and the dextral shear zones, which makes an average of 122°. The bisecting angle of 61° was used as the average angle between the shear planes and the direction of the maximum shortening (S_1). Then for each shear zone the orientation of the extension (T) and the shortening axes (P) was calculated from the orientation of the shear plane (C plane) and the stretching lineation using the above mentioned angle of 60° between S_1 and the stretching lineation. For the calculations a PC program published by Sperner *et al.* [1993] has been used.

The mean strain directions (Figure 2c) in the strike-slip shear zones gave a NW-SE direction of the maximum shortening direction (S_1), a NE-SW direction of extension axis (S_3), and a vertical intermediate strain axis (S_2). The thrusting shear zones revealed a NW-SE orientation of S_1 , a NE-SW orientation of S_2 , and a subvertical attitude of S_3 . Thus both sets of shear zones gave a NW-SE direction for the maximum horizontal shortening axes.

3.1.1.3. Folds: Locally, the pervasively foliated rocks as well as subhorizontal quartz-feldspar veins show upright folds with subhorizontal NE-SW trending axes (Figure 2b). The folds are symmetrical and moderately closed. The NE-SW direction of fold axes is also compatible with a NW-SE orientation of the horizontal shortening axes.

3.1.2. Age of the structures. Isotope age data (Tables 1 and 2) indicate that the fully ductile structures of the Bolfin Complex were formed in Early to Middle Jurassic times: The intrusion age of the igneous protolith of the Bolfin Complex from Mejillones Peninsula can be inferred from a Rb-Sr whole rock age of 200 ± 10 Ma [Díaz *et al.*, 1985] and U-Pb zircon ages of 196 ± 4 and 191 ± 6 Ma [Damm *et al.*, 1986]. The minimum age of the pervasive foliations is given by a U-Pb zircon age of 174 ± 16 Ma obtained from a granite which intruded the amphibolitic mylonites east of Antofagasta (Las-Toscas granite) [Damm *et al.*, 1986]. The upper age limit of the semiductile conjugate shear zones can be inferred from K-Ar age determinations of hornblende porphyroclasts (165 ± 5 and 157 ± 6 Ma; Table 1); the lower age limit is given by K-Ar cooling ages of postdeformative biotite of 155–152 Ma. These age values match the $^{40}\text{Ar}/^{39}\text{Ar}$ and Rb-Sr age data published by Scheuber *et al.* [1995] from high-grade shear zones south of Antofagasta (hornblende circa 153 Ma and biotite circa 150 Ma).

3.1.3. Nonmetamorphic structures. Nonmetamorphic structures indicate a kinematic regime similar to the described high-temperature structures of the Bolfin Complex. These structures, which comprise folds, thrusts, and other brittle faults, have been studied in detail in various places (Michilla, north of Paposo and south of Taltal; Figure 2).

3.1.3.1. Folds and thrusts: Folds are rather scarce in the Coastal Cordillera mainly owing to the prevailing lithology of the rocks: thick, massive lavas and intrusive rocks which, in many cases, are not suitable for folding. However, in some places, for example, ~20 km south of Taltal and 5 km SE of Michilla, well-stratified folded rocks occur (Figure 4b), comprising Upper Triassic continental sediments, Lower Jurassic marine sediments, and tuffs within the Jurassic volcanics. The folds generally have nearly horizontal ENE to NE trending axes and vertical to steeply dipping axial planes (Figure 2d). As these folds are confined to

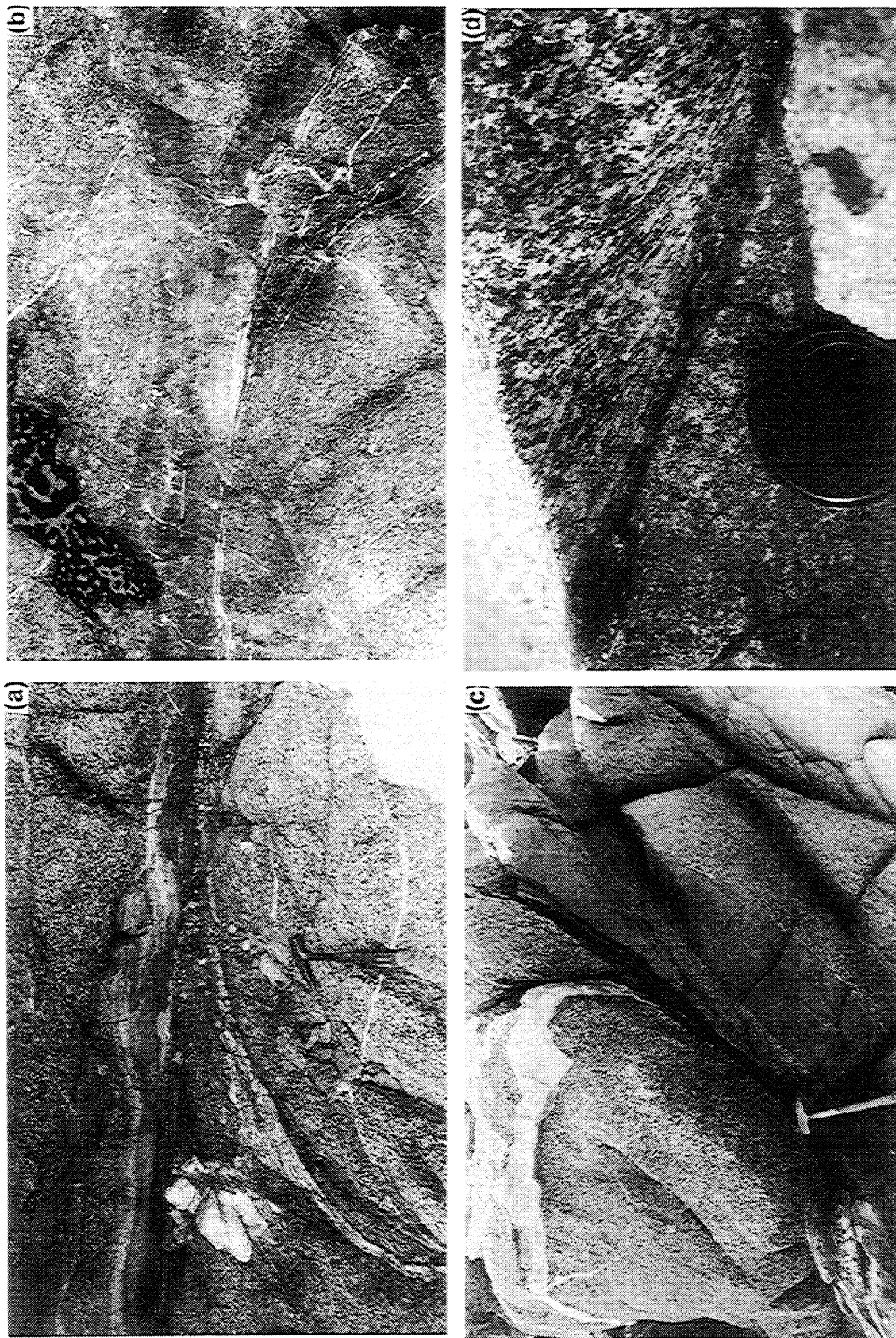


Figure 3. Discrete shear zones cutting the foliated amphibolitic gneisses of the Bolfin Complex: (a) ENE-WSW trending dextral shear zone; (b) N-S trending sinistral shear zone; (c) thrust shear zone with vergence toward SE; note the transposition of the quartz-feldspar vein and the deformed amphibolitic dike in the central part; and (d) discrete thrust with vergence toward NW.

the N-S trending magmatic arc, they are arranged in an en echelon manner and thus match the overall sinistral regime. Brittle thrusts also strike ENE-WSW to NE-SW, indicating the same sinistral, arc-parallel strike-slip regime as the folds do. The orientations of thrusts and folds indicate a NW-SE directed shortening direction, which has also been inferred from the discrete shear zones of the Bolfin Complex.

The upper age limit of folding and thrusting is given by the age of the youngest marine strata conformably overlying the Jurassic volcanics which are late Callovian in age [Kossler, 1996] (according to Gradstein *et al.* [1994], circa 159 ± 4 Ma). This age is in agreement with a K-Ar hornblende age of 155 ± 5 Ma obtained south of Taltal from a sill (Table 1) which intruded into Lower Jurassic strata and which was subject to thrusting. The lower age limit is given by K-Ar whole rock age data of 149 ± 4 Ma of a gabbroic stock which cuts the tilted and folded strata near Michilla (Table 2) [Astudillo, 1984] and K-Ar ages of circa 147 Ma of a mafic dike from a dike swarm cutting the folded strata without being tilted (see section 3.1.3.2). Thus folding and thrusting occurred between circa 155 and 150 Ma, i.e., during the same time span as the formation of the discrete shear zones.

3.1.3.2. Faults: Brittle faults other than thrusts are abundant in the Coastal Cordillera. However, as faulting occurred several times from Jurassic to Recent, it is difficult to distinguish arc structures (Jurassic-Early Cretaceous) from younger structures which formed in different stress regimes when the Coastal Cordillera was subject to forearc deformations [e.g., Hervé, 1987; Armijo and Thiele, 1990]. Faults are assumed to be Jurassic-Early Cretaceous in age when they are hydrothermally mineralized, because mineralization took place during that time in the Coastal Cordillera [Boric *et al.*, 1990]. The same holds if the faults are intruded by Late Jurassic dikes, a situation that has been observed in some places, for example, south of Taltal.

The orientations of fault planes and slickenside striations of probable Late Jurassic-Early Cretaceous age have been measured at Michilla and south of Taltal. Paleostress directions have been obtained using the right-dihedra method of Angelier and Mechler [1977] and Angelier [1994] using the computer program "Geofuge 6" [Wallbrecher and Unzog, 1997]. The results are shown in Fig 2: Faulting is dominated by strike-slip and normal faulting kinematics with a NW-SE to NNW-SSE orientation of the maximum horizontal shortening axis (S_H). This direction agrees with the shortening direction of the folds and thrusts and of the ductile structures of the Bolfin Complex.

3.2. Stage II: Extensional Structures and Magmatic Growth of the Arc

Arc-normal crustal extension occurred after volcanism had ceased in Callovian times [Kossler, 1996]. At plutonic levels, extension was accommodated by the emplacement of large volumes of calcalkaline plutons whereas normal faulting occurred at the level of the volcanics which generally display homoclinal tilting of ~30° - 70° toward westerly directions north of 25°S and toward easterly directions south of 25°S. It is important to note that this tilting is restricted to the volcanic level whereas the originally horizontal or vertical attitude of planar structures of the deep crustal Bolfin Complex (older than 165 Ma) is preserved.

The basement underlying the volcanics can only very rarely be observed; instead, in most cases the volcanics are intruded by extended calcalkaline plutons. The observation that the flat roofs of these plutons unconformably cut the tilted volcanics indicates that the plutons are younger than tilting. This is in agreement with radiometric ages of the plutonics of less than 165 Ma. Typically, the plutons form N-S elongate bodies which are >50 km long and

5-20 km wide [e.g., Marinovic *et al.*, 1995]. According to the Al-in-hornblende geobarometer of Schmidt [1992] the load pressure during the crystallization of hornblende within the plutons was 200-300 MPa, which corresponds to an intrusion level of less than 6-9 km [González, 1996].

At the top of the plutonic level it can be observed that N-S trending brittle normal faults grade into ductile normal-faulting shear zones, which are common along the contact between the calcalkaline plutonic bodies and the tilted arc volcanics (Figures 2 and 5). Within these shear zones, strongly deformed amphibolitic mylonites occur [cf. Brown *et al.*, 1991], which laterally grade into undeformed volcanics. A normal-faulting kinematic regime in these shear zones is revealed by kinematic indicators such as asymmetric extensional crenulation cleavages, sigmoidal structures, and sheath folds (Figure 5). The N-S trend of the normal faults, stretching lineations steeply plunging to the east, and the westerly dip of the volcanic blocks suggest that tilting of the volcanic pile and movements along the ductile normal faults were linked tectonic processes which indicate an asymmetrical arc-normal crustal stretching.

At the nonmetamorphic sedimentary crustal level, low-angle normal faults have been found in several places (Paposo, south of Taltal; Figures 4b and 4c). They bring in contact Middle Jurassic volcanics over Lower Jurassic marine sediments, i.e., younger over older rocks. In one case a listric bending of the normal fault can be observed (Figure 4b) whereas in other cases the faults occur only as flat planes. Kinematic indicators such as cleavage or bedding planes which are bent into the fault planes show a movement of the hanging wall toward west or east, thus indicating arc-normal extension.

The maximum age of the extension is given by the upper Callovian age of the uppermost arc volcanics [Kossler, 1996], which corresponds to the age of those plutons which intruded the volcanic pile and which are younger than 165-160 Ma. Biotite of mylonites from a ductile normal fault show a K-Ar cooling age of 152 ± 4 Ma (Table 1), which gives the minimum age of the extension.

3.3 Stage III: Oblique Dilation and Intrusion of Dikes

In the brittle crust, dikes generally propagate along planes oriented perpendicularly to the least principle stress, and the strike of dikes represents the least horizontal stress S_H [Delaney *et al.*, 1986; Emerman and Marrett, 1990; Price and Cosgrove, 1990; Zoback, 1992; Thomas and Pollard, 1993]. In order to obtain information about stress directions, we have measured the orientation and thickness of Late Jurassic mafic dikes mainly along four sections through the Coastal Cordillera (Figure 2) but also between these sections. So orientation data exist over ~400 km of the arc from 22°S to 25°45'S; they are shown in Figure 6a ($n = 1190$, average thickness is 3.4 ± 1.7 m). The strike of the generally very steep to vertical dikes displays a considerable scatter ranging from NE-SW through N-S to NW-SE; E-W trending dikes are rare. However, a closer inspection of single sections shows that the scatter in the orientation is due to the existence of at least two dike systems; one trending NE-SW to ENE-WSW and another one trending N-S to NW-SE. In numerous places, crosscutting relationships between dikes show that NE-SW trending dikes are cut by NW-SE to NNW-SSE trending dikes (Figure 4d). The average angle between both dike generations is ~70°-90°. In Section D (south of Taltal) also an intermediate generation striking N-S can be distinguished. The observation of the crosscutting relations between the dike generations clearly indicates that the dikes intruded during at least two episodes with contrasting directions of S_H . During the intrusion of the older

Table 1. Results of K-Ar Age Determinations for This Study From the Coastal Cordillera

Locality	Material Dated	K, %	⁴⁰ K, ppm	⁴⁰ Ar/ ³⁹ Ar Total	⁴⁰ Ar, ppm	Age, Ma	Remarks
<i>Plutonic Rocks (Quartz Diorites, Including the Bofin Complex) Containing NE and NW Striking Dikes</i>							
23°06.449'S, 70°30.097'W	hornblende	0.381	0.455	0.5955	0.004687	169 ± 6	
23°14.072'S, 70°16.045'W	biotite	5.897	7.035	0.8265	0.06477	152 ± 3	
25°44.010'S, 70°33.445'W	hornblende	0.141	0.168	0.309	0.001769	172 ± 8	
25°38.787'S, 70°31.650'W	hornblende	0.299	0.357	0.4925	0.003551	164 ± 6	
<i>Discrete Shear Zones (Greenschist Facies Mylonites)</i>							
23°30.046'S, 70°63.927'W	hornblende	0.686	0.818	0.5515	0.08213	165 ± 5	dextral ENE-WSW striking shear zones
23°30.046'S, 70°63.927'W	biotite	6.516	7.773	0.8415	0.0729	155 ± 3	dextral ENE-WSW striking shear zones
23°30.046'S, 70°63.927'W	hornblende	0.405	0.483	0.359	0.04611	157 ± 6	sinistral N-S striking shear zones
23°30.046'S, 70°63.927'W	biotite	6.419	7.568	0.818	0.07006	151 ± 3	sinistral N-S striking shear zones
<i>Early Cretaceous Granodiorites Containing Only NW Trending Dikes</i>							
23°14.125'S, 70°18.261'W	hornblende	0.239	0.285	0.432	0.002402	140 ± 5	
23°14.125'S, 70°18.261'W	biotite	6.754	8.057	0.8345	0.06863	141 ± 3	
<i>Early Cretaceous Granodiorites Without Dikes</i>							
25°28.080'S, 70°19.787'W	hornblende	0.515	0.614	0.576	0.004940	133 ± 5	
25°31.306'S, 70°19.344'S	hornblende	0.341	0.406	0.450	0.003330	136 ± 5	
<i>Ductile Normal Fault</i>							
23°31.904'S, 70°06.063'W	biotite	7.309		0.818	0.07006	152 ± 4	sheared Jurassic lava
<i>Sheet-Like Andesitic Intrusions</i>							
25°38.220'S, 70°33.543'W	hornblende	0.451	0.538	0.4609	0.005067	155 ± 5	sill
23°12.732'S, 70°17.109'W	hornblende	0.308	0.367	0.3645	0.003263	147 ± 6	NW striking dike
23°14.125'S, 70°18.261'W	secondary hornblende	0.274	0.327	0.4765	0.002886	146 ± 5	NE striking dike

Table 2. Age Data From Literature

Reference	Locality	Material	Rock Type	Method	Age, Ma
<i>Plutonic Rocks (Including the Bofin Complex) Containing NE and NW Trending Dikes</i>					
Díaz <i>et al.</i> [1985]	23°25.2'S, 70°35.3'W	whole rock	gabbro to granite	Rb-Sr	200 ± 10
Damm <i>et al.</i> [1986]	23°25'S, 70°35'W (approx.)	Zircon	gabbro	U-Pb	196 ± 4
Damm <i>et al.</i> [1986]	23°28'S, 70°34'W (approx.)	Zircon	gabbro	U-Pb	191 ± 6
Astudillo [1984]	22°40.2'S, 70°09.8'W	whole rock	gabbroic stock	K-Ar	154 ± 8
Astudillo [1984]	22°40.2'S, 70°09.8'W	whole rock	gabbroic stock	K-Ar	149 ± 4
Scheuber <i>et al.</i> [1995]	24°11.450'S, 70°25.480'W	hornblende	gabbro	⁴⁰ Ar/ ³⁹ Ar	152.9 ± 2.4
<i>Late Jurassic-early Cretaceous plutons containing only NW-trending dikes</i>					
Hervé and Marinovic [1989]	24°07.7'S, 70°22.8'W	whole rock	tonalite	Rb-Sr	145 ± 10
Hervé and Marinovic [1989]	24°40.8'S, 70°29.6'W	biotite	granodiorite	K-Ar	144 ± 4
Hervé and Marinovic [1989]	24°11.082'S, 70°10.002'W	biotite	diorite	K-Ar	147 ± 4
Hervé and Marinovic [1989]	24°40.800'S, 70°29.550'W	biotite	granodiorite	K-Ar	144 ± 4
<i>Early Cretaceous Plutons Without Dikes</i>					
Maksaev [1990]	23°14.1'S, 70°17.5'W	hornblende	tonalitic stock	⁴⁰ Ar/ ³⁹ Ar	137 ± 2.2
Scheuber <i>et al.</i> [1995]	24°38.3'S, 70°20.6'W	hornblende	granodiorite	⁴⁰ Ar/ ³⁹ Ar	138.0 ± 1.7
<i>Ductile Normal Fault In Jurassic Volcanics</i>					
Hervé and Marinovic [1989]	24°22.53'S, 70°26.76'W	whole rock	mylonite (andesitic lava)	K-Ar	139 ± 5
<i>Dikes</i>					
Chavez [1985]	23°25.5'S, 70°09.8'W	hornblende	andesite	K-Ar	149 ± 13
Maksaev [1990]	23°14.66'S, 70°18.75'W	hornblende	andesite	⁴⁰ Ar/ ³⁹ Ar	148.5 ± 1
Chavez [1985]	23°24.168'S, 70°10.002'W	hornblende	andesite	K-Ar	147 ± 13
Maksaev [1990]	25°5.502'S, 70°29.100'W	plagioclase	andesite	K-Ar	139 ± 5
Maksaev [1990]	22°04.752'S, 70°09.918'W	hornblende	andesite	⁴⁰ Ar/ ³⁹ Ar	139.8 ± 7.7
Dallmeyer <i>et al.</i> [1996]	26°33.833'W, 70°39.400'S	whole rock	basaltic andesite	⁴⁰ Ar/ ³⁹ Ar	155.5 ± 0.6
Dallmeyer <i>et al.</i> [1996]	26°22.433'S, 70°26.483'W	whole rock	basaltic andesite	⁴⁰ Ar/ ³⁹ Ar	153.7 ± 0.7
Dallmeyer <i>et al.</i> [1996]	26°28.400'S, 70°23.883'W	whole rock	basaltic andesite	⁴⁰ Ar/ ³⁹ Ar	142.1 ± 0.9
Dallmeyer <i>et al.</i> [1996]	26°22.483'S, 70°29.300'W	whole rock	basaltic andesite	⁴⁰ Ar/ ³⁹ Ar	129.2 ± 0.5

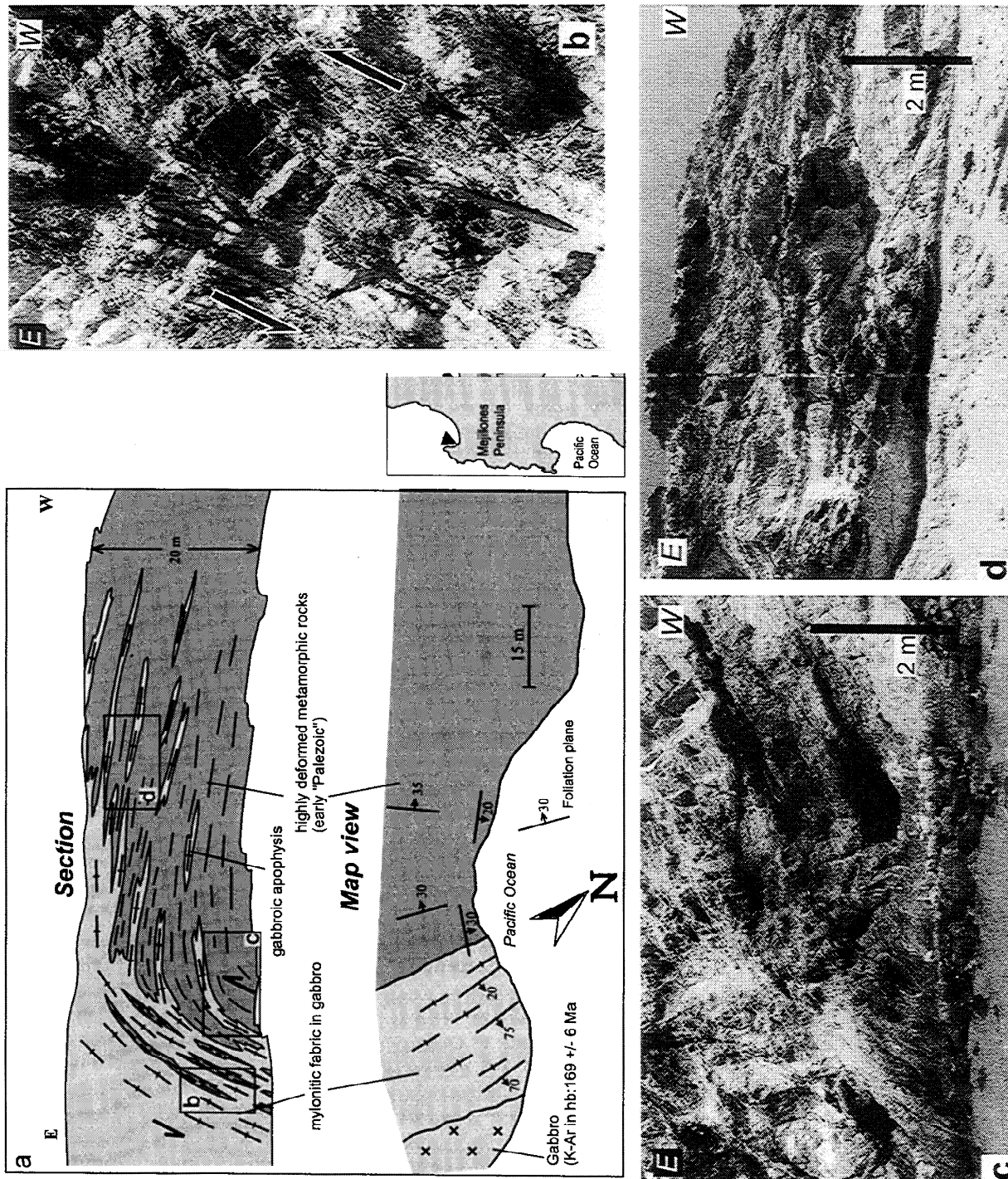


Figure 5. Ductile normal fault in northernmost Mejillones Peninsula. (a) E-W section and map view. A Jurassic gabbro (K-Ar in homblende: 169 ± 6 Ma) in contact with early Paleozoic micaschists containing apophyses of the gabbro is shown. The foliation planes of the micaschists and the apophyses form a drag fold, and mylonitic fabrics developed along the gabbro contact. (b-d) Photographs showing kinematic indicators of the mylonites. These indicators give evidence of normal faulting along the contact.

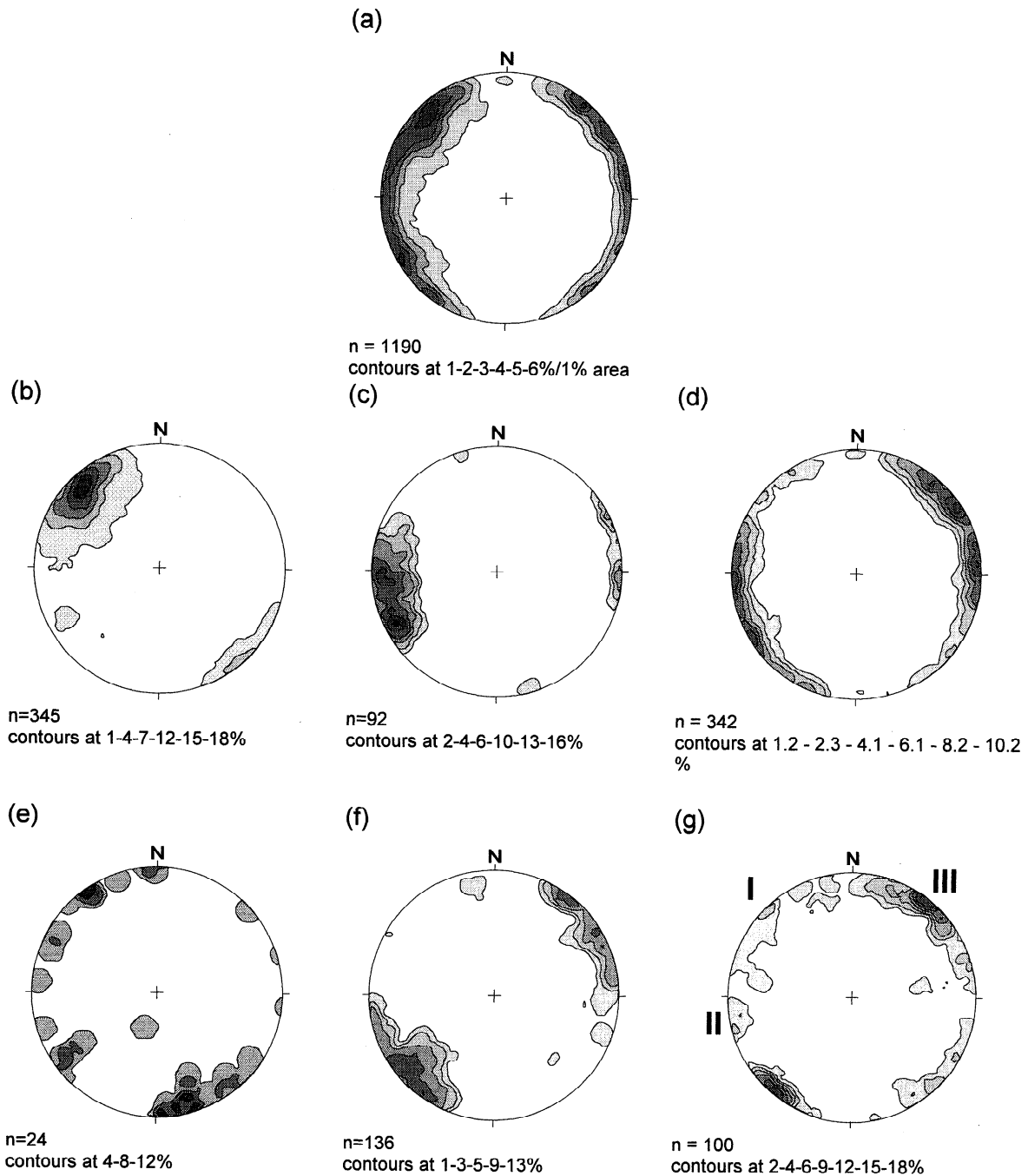


Figure 6. Contoured pole figures of dike orientations in the Coastal Cordillera (equal area, lower hemisphere projection; for location of the sections, see Figure 2a). (a) Diagram containing all measured andesitic dikes from the Coastal Cordillera. (b) Section A, andesitic dikes in Middle to Late Jurassic (160 Ma) diorite containing NE- and NW trending dikes. (c) Section A, andesitic dikes in late Jurassic (145 Ma) tonalite containing only NW-SE to NNW-SSE trending dikes. (d) Section B, andesitic dikes in Middle Jurassic diorites. (e) Section C, andesitic dikes in Middle to Late Jurassic diorite. (f) Section C, andesitic dikes in Late Jurassic granodiorite. (g) Section D, andesitic dikes in Paleozoic to Lower Jurassic rocks. Three generations of dikes can be distinguished by criteria of crosscutting in the field, NE-SW trending dikes (generation I) are oldest, ~N-S trending dikes (generation II) are intermediate, and NW-SE trending dikes (generation III) are youngest.

dikes it was oriented NE-SW and then changed over a N-S direction to NW-SE during the intrusion of the younger dikes.

The age of the dikes can be inferred from their contact relations and from isotope age data (Tables 1 and 2): The dikes of both generations cut and postdate deformation of the discrete shear zones as well as the folds and thrusts described above, which are older than 155 Ma and thus give an upper age limit for the dikes of both generations. From field observations the ages of the NE-SW trending dikes also can be distinguished from those of the NW-SE trending dikes: In various places the plutons containing dikes of all generations (NE- and NW trending) are cut by plutonic bodies containing only NW trending dikes or no dikes at all (section A in Figures 6b and c and section C in Figures 6e and 6f; see Tables 1 and 2). The plutons containing only NW trending dikes have ages of circa 144-147 Ma (e.g., the Cerro Cristales Pluton; in Figure 7; Rb-Sr whole rock age of 145 ± 10 Ma and a K-Ar biotite age of 146 ± 4 Ma) [Hervé and Marinovic, 1989]. Plutons without dikes are generally younger than 140 Ma; for example, the Remiendos Pluton ($^{40}\text{Ar}/^{39}\text{Ar}$ in hornblende: 138 ± 1.4 Ma) [Scheuber *et al.*, 1995], cropping out east of the Atacama Fault Zone between 24° and 25°S , does not contain any dike. These contact relations of the dikes seem to be a more reliable criterion for establishing their age than isotope age datings are, because in many cases the dikes were subject to thermal overprinting and/or hydrothermal alteration, which resulted in age resetting. However, the age range reported is also consistent with a K-Ar hornblende age of 147 ± 6 Ma determined in a NW-SE trending dike north of Antofagasta (Table 1) and also with most of the age values reported in the literature (Table 2). From all the age constraints it can be concluded that the NE-SW trending dikes intruded between ~ 155 and 147 Ma and that the NW-SE dikes intruded between ~ 147 and 140 Ma.

There are two possible explanations for the existence of two dike generations, either a rotation of the principal stresses or a rotation of blocks in a constant stress regime. We think that the second possibility can be ruled out for two reasons:

1. Paleomagnetic data reported by various authors suggest a clockwise rotation of $\sim 25^\circ$ - 30° of big parts of the central Andes south of 18°S [Roperch and Carlier, 1992; Riley *et al.*, 1993; Aubry *et al.*, 1996; Randall *et al.*, 1996], which is been attributed to either a rotation of the whole central Andean domain due to oroclinal bending or to the rotation of single blocks due to strike-slip faulting [Forsythe and Chisholm, 1994]. However, as this rotation affected rocks from Triassic to Tertiary in age, it must have occurred in Cenozoic times and has nothing to do with the orientation of Late Jurassic-Early Cretaceous dikes. Furthermore, new paleomagnetic data [Roperch *et al.*, 1997] show that the rotation of the Coastal Cordillera was not uniform but subject to changes along strike: Between 22° and 23.5°S there was essentially no rotation at all whereas south of 23.5° there was a clockwise rotation of $\sim 30^\circ$. However, regardless of the magnetic rotations, the dikes show similar orientations all over the Coastal Cordillera from 22° to 26°S . Thus no evidence for a Late Jurassic 70° - 90° rotation of blocks can be inferred from paleomagnetic data.

2. The angular relationship between the two dike generations (70° - 90°) is fairly constant in all sections; in the case of local block rotations this would mean that all blocks should have rotated more or less the same amount, which also seems rather unlikely. However, the rotation of single blocks of $\sim 30^\circ$ after the intrusion of the younger (NW trending) dikes seems possible. One notable example of possible block rotations is the northern part of Mejillones Peninsula (section A in Figures. 2 and 6c), where the older dikes strike E-W but the younger dikes strike N-S. How-

ever, the angle between both generations of dikes ($\sim 70^\circ$ - 90°) is the same as that in the other sections.

3.4 Stage IV: Younger Sinistral Movements Parallel to the Arc

Starting with the emplacement of the NW-SE trending dikes, sinistral strike-slip movements prevailed in the Coastal Cordillera along the >1000 km long, arc-parallel Atacama Fault Zone (Figures. 2 and 7a). A sinistral sense of shear can be inferred from many mylonitic structures along this fault zone (for a detailed description see the work of Scheuber and Andriessen, [1990]). The $^{40}\text{Ar}/^{39}\text{Ar}$ and Rb-Sr datings of mylonites gave a deformation age of ~ 125 Ma [Scheuber *et al.*, 1995]. Dikes and small plutonic bodies were displaced with a sinistral sense (Figure 7b) along brittle faults of the Atacama Fault Zone where it cuts the rocks of the Bolfin Complex.

4. Discussion and Conclusions

The observations reported in sections 1-3 show that the Jurassic-Early Cretaceous magmatic arc was subject to strong deformations which were closely related to magmatic activity. This relationship can, for example, be shown by the observation that tectonic movements were accommodated by the opening and intrusion of dikes and other plutonic bodies; furthermore, when magmatism ceased at ~ 120 Ma [Andriessen and Reutter, 1994], deformations also ended in the Coastal Cordillera. Ductile deformation was possible at moderate depths (<10 km) owing to magmatic heat supply resulting in intense weakening of the crust [Grocott *et al.*, 1994; Scheuber, 1994; González, 1996]. This weakening was further enhanced by melts which facilitated deformation, as can be inferred from syntectonic leucocratic veins and mafic dikes which intruded along the shear planes and which were also sheared (Figures 3a-3c). This process corresponds to "melt-enhanced deformation" [Hollister and Crawford, 1986]. Crustal weakening resulted in the concentration of deformation on the magmatic arc, which is shown by the fact that at same time as the arc underwent strong deformations, there was tectonic quiescence in the backarc basin bordering the arc to the east [Prinz *et al.*, 1994].

The fact that the Jurassic-Early Cretaceous arc and backarc had the same N-S trend as that of the present trench allows us to infer the kinematic pattern of the converging plates from the tectonic structures of the arc. We interpret the magmatic arc as a mega shear zone in the structures of which the movements of the forearc sliver relative to the backarc are recorded.

According to the kinematic reconstructions presented in section 3, we are able to identify the described four deformational stages in the evolution of the magmatic arc (Figure 8). These stages can be interpreted in terms of movements of the forearc sliver: During stage I (circa 195-155 Ma) it moved toward south, resulting in NW-SE shortening and sinistral strike-slip motions within the arc. During stage II (circa 160-150 Ma) the input of large volumes of magmas into the arc's crust was accompanied by strong arc-normal extension, which resulted in a movement of the forearc sliver toward the trench. During stage III (155-140 Ma), arc-normal extension was replaced by oblique extension indicated by the intrusion of dikes. The existence of two sets of dikes indicates a change of the direction of S_H from NW-SE to NE-SW and back to NW-SE. During stage IV, sinistral forearc movements led to the formation of low-temperature mylonites and cataclases along the AFZ.

In parts, this tectonic history corroborates the Jurassic-Early Cretaceous geodynamic reconstructions of the SE Pacific adja-

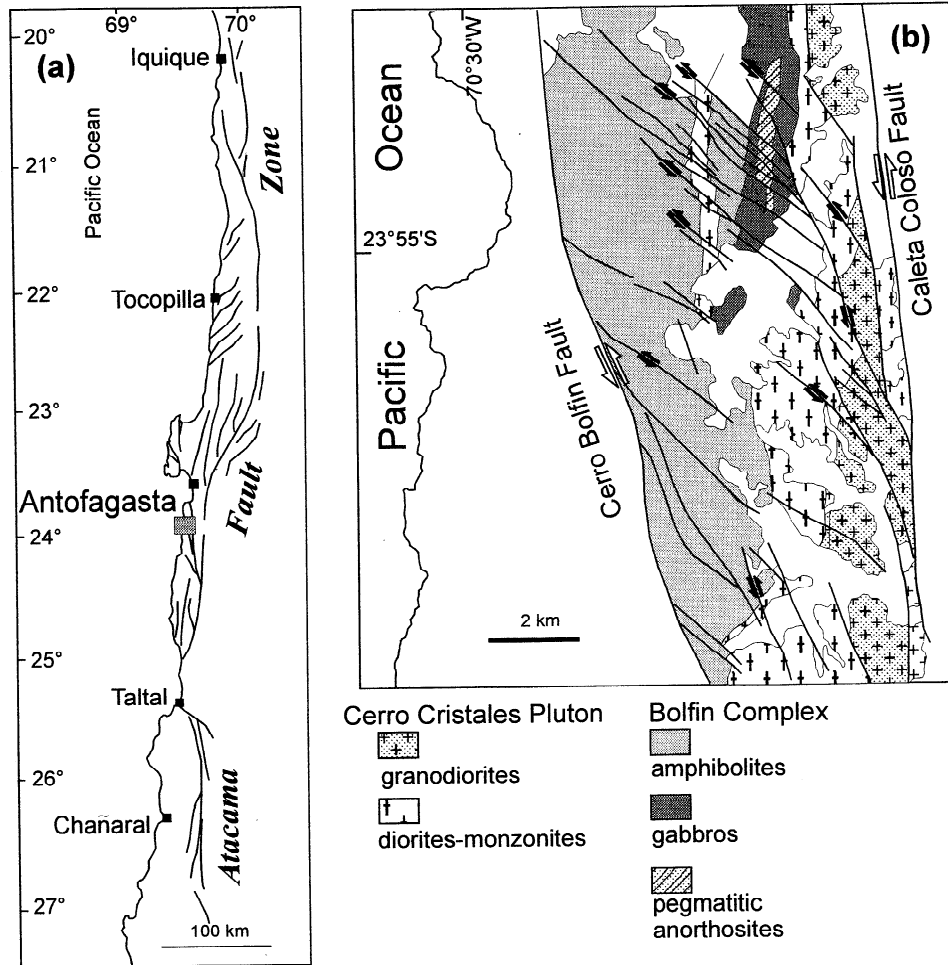


Figure 7: (a) The Atacama Fault Zone in northern Chile. (b) Geological sketch map of the Coastal Cordillera south of Antofagasta showing the distribution of the Bolfin Complex, the Cerro Cristales Pluton, two major faults of the Atacama Fault Zone (Caleta Coloso Fault and Cerro Bolfin Fault), and related sinistral displacements in Jurassic igneous rocks.

cent to South America depicted in Figure 1 which indicate strongly oblique, SE directed convergence which was probably related to a NE-SW trending spreading center that controlled the separation between North America and South America (Thetys model of *Jaillard et al.*, [1990]). The southward motions of the forearc sliver are compatible to this plate configuration during stages I, IIIb, and IV. However, the kinematic patterns of stages II and IIIa apparently contradict this configuration.

The kinematic patterns of stages I, IIIb, and IV correspond to arc-forearc tectonics observed in many modern high-stress subduction zones where the forearc moves with the same sense as convergence obliquity (e.g., Sumatra [*Fitch*, 1972], and the Aleutians [*Geist and Scholl*, 1992]). The deformations in these zones are caused by seismic coupling between the plates that allow the transmission of the S_H vector, which is oriented parallel to the vector of plate convergence, from the subduction zone into the magmatic arc. This coincidence of S_H and the vector of plate motion is also consistent with observations of the present-day stress fields where there is a worldwide agreement between these vectors (first-order stress field) [*Zoback*, 1992].

For the arc-normal extension of stage II, strong seismic coupling between the plates can be ruled out. One possible explanation for the extensional regime could be a change from a high-stress to a low-stress subduction style. Low-stress subduction [*Uyeda and Kanamori*, 1979; *Royden*, 1993] implies a fast foundering of the subducting plate and thus an increased rollback rate of the trench (e.g., Mariana subduction zone). Such a process was suggested previously for the Jurassic evolution of the Coastal Cordillera magmatic arc by *Grocott et al.* [1994].

The oblique, NW-SE directed extension of stage IIIa (Figure 8c) is very difficult to explain in a system of sinistral plate convergence. We think of three possible mechanisms which, however, at the moment cannot be proven by geological data. One possible reason for NW-SE extension could be that there was a different plate configuration adjacent to South America; that is, a short-term reorganization of the plate system could have taken place, and an extra plate was present, which has been completely subducted. Although this possibility cannot be ruled out, it seems to be rather unlikely since the reversals occurred during a relatively short time (155-147 Ma) in an otherwise uniform history of

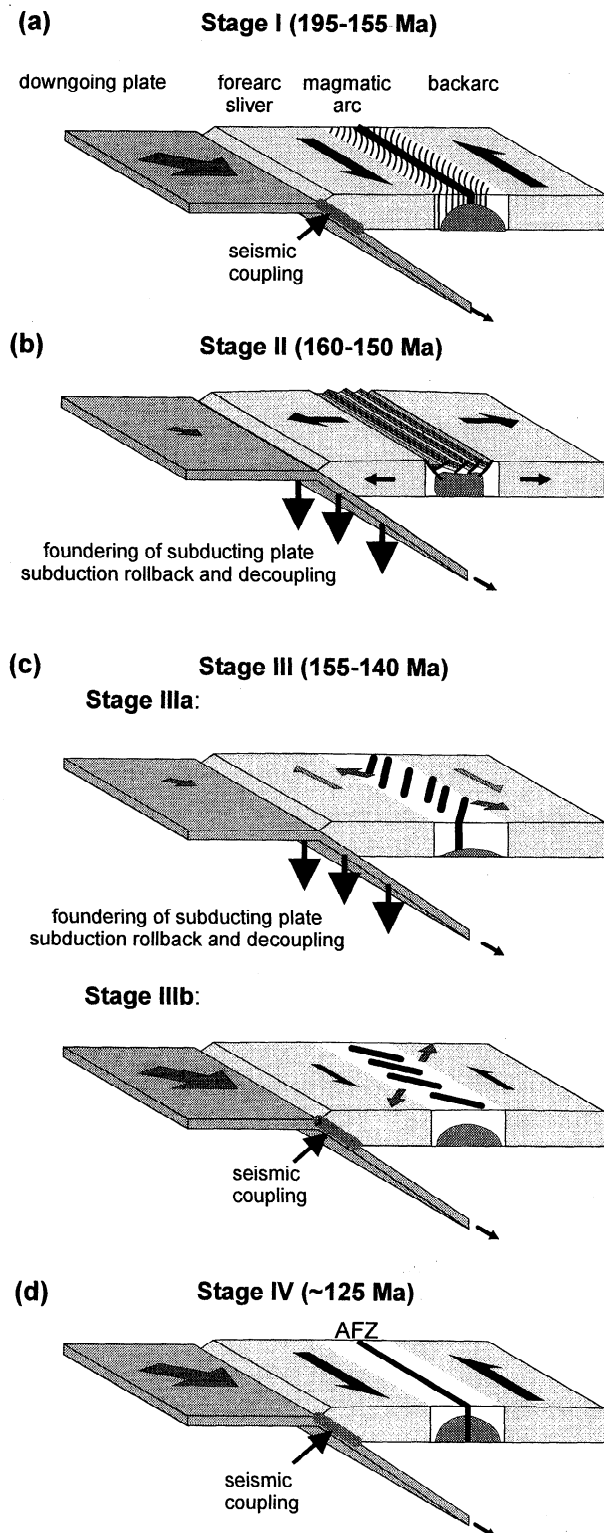
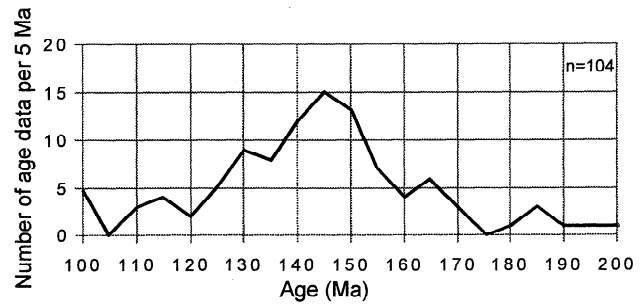


Figure 8: Model for the tectonic evolution of the Jurassic-Early Cretaceous arc of north Chile and the inferred subduction zone regime. (a) Stage I: volcanism and deep-seated plutons together with older sinistral movements in a high-stress subduction regime indicating a high degree of seismic coupling between the plates. (b) Stage II: intense shallow-level plutonism without volcanism, magmatic crustal growth and arc-normal extension, and decoupling between the plates (low convergence rate) indicating low-



TECTONICS.18.5p908f9

Figure 9. Frequency distribution of biotite age data (K-Ar, $^{40}\text{Ar}/^{39}\text{Ar}$, and Rb-Sr) of plutonic rocks from north Chile. The peak at 150-140 Ma indicates cooling of the arc's crust below 300°C (source includes 60 authors, compilation of *Maksav* [1990] and *Scheuber* [1994]).

sinistral motion of the forearc sliver. It would mean that convergence toward the SE was active before 155 Ma; then, over a period of some 8 Myr, NE directed subduction occurred, which afterwards was replaced again by the southeastward directed convergence with about the same direction as that before the reversal. A second possibility could be an oblique corner flow pushing the forearc toward north. The work of *Furukawa* [1993a, b] has shown that corner flow is able to produce considerable differential stresses (>100 MPa) at the base of the upper plate. Maximum stresses are vertical beneath the arc and become horizontal beneath the forearc. These vertical maximum stresses could be able to produce horizontal extension in the arc, although it seems difficult to drag the forearc sliver in a direction opposite to convergence, because the surface contact between the asthenospheric wedge and the forearc is rather small, and so the shear stresses below the forearc would also be low. A third possibility would imply that first elastic strain accumulated in the upper plate with an oblique shortening direction caused by oblique convergence. Because of a decrease in convergence rate, this elastic strain could have been released, resulting in the formation of the NE-SW trending dikes (stage IIIb in Figure 8c). The accumulation of sufficient amounts of elastic strain requires that the arc's crust behaved in a rigid manner, which was not the case during intense magmatism. However, when there is a magmatic lull, the arc's upper crust cools down rapidly (less than 1 Ma) [*Barton and Hanson*, 1989] resulting in an increase of crustal strength, which in turn increases the ability to accommodate elastic strain. The distribution of biotite ages in plutons of the Coastal Cordillera (Figure 9) shows a peak of cooling below 300°C at circa 150 Ma, which gives a hint that big parts of the arc's upper crust had cooled down beneath the temperatures for the onset of quartz ductility, which means that the upper crust had become rigid enough to build up elastic strain.

The results reported in this paper have interesting bearings on the kinematic and geodynamic interpretation of structures of an-

stress subduction. (c) Stage III: oblique dilatation in the arc. Stage IIIa: intrusion of NE-SW trending dikes (NW-SE extension) indicating decoupling in a low-stress subduction regime. Stage IIIb: intrusion of the NW-SE trending dikes (NE-SW extension) point to a high coupling in a high-stress subduction regime. (d) Stage IV: sinistral displacement along Atacama Fault Zone (AFZ) also indicating a high degree of coupling in a high-stress subduction regime.

cient orogens. In many cases these orogens have passed through a stage in which a magmatic arc developed (e.g., Variscides, Krohe, 1991). From the arc structures inferences are often made about ancient plate motions. However, this is not possible in all cases, because the arc structures may show kinematic patterns which are opposed to plate convergence.

References

- Andrews, D.J., Numerical simulation of sea-floor spreading, *J. Geophys. Res.*, **77**, 6470-6481, 1972.
- Andriessen, P.A.M., and K.-J. Reutter, K-Ar and fission track mineral age determinations of igneous rocks related to multiple magmatic arc systems along the 23°S latitude of Chile and NW Argentina, in *Tectonics of the Southern Central Andes*, edited by K.-J. Reutter, E. Scheuber, and P. Wigger, pp. 141-153, Springer-Verlag, New York, 1994.
- Angelier, J., Tectonic analysis of fault slip data sets, *J. Geophys. Res.*, **89**, 5835-5848, 1984.
- Angelier, J., Fault slip analysis and paleostress reconstruction, in *Continental Deformation*, edited by P.L. Hancock, pp. 53-100, Pergamon, Tarrytown, N.Y., 1994.
- Angelier, J., and P. Mechler, Sur une méthode graphique de recherche des contraintes principales également utilisable en tectonique et en séismologie: La méthode des dièdres droits, *Bull. Soc. Geol. Fr.*, **7**, 1309-1318, 1977.
- Arabas, W.J., Geological and geophysical studies of the Atacama fault zone in northern Chile, Ph.D. thesis, 264 pp., Calif. Inst. of Technol., Pasadena, 1971.
- Armijo, R., and R. Thiele, Active faulting in northern Chile: Ramp stacking and lateral decoupling along a subduction plate boundary, *Earth Planet. Sci. Lett.*, **98**, 40-61, 1990.
- Astudillo, O., Geología y metalogénesis del distrito minero Carolina de Michilla, Antofagasta, II Región, Chile, B. Sc. thesis, 131 pp., Universidad del Norte, Antofagasta, Chile, 1984.
- Aubry, L., P. Roperch, M. de Urreizieta, E. Rosello, and A. Chauvin, Paleomagnetic study along the southeastern edge of the Altiplano - Puna Plateau: Neogene tectonic rotations, *J. Geophys. Res.*, **101**, 17,883-17,899, 1996.
- Barton, M.D., and L.B. Hanson, Magmatism and the development of low-pressure metamorphic belts: Implications from the western United States and thermal modeling, *Geol. Soc. Am. Bull.*, **101**, 1051-1065, 1989.
- Boric, R., F. Diaz, and V. Makshev, Geología y yacimientos metalíferos de la Región de Antofagasta, 246 pp., Serv. Nac. Geol. Miner., Boletín No. 40, Santiago, Chile, 1990.
- Brown, M., F. Diaz, and J. Grocott, Displacement history of the Atacama fault system 25°00'S-27°00'S, northern Chile, *Geol. Soc. Am. Bull.*, **105**, 1165-1174, 1993.
- Brown, M., F. Diaz, and J. Grocott, Atacama fault system: History of displacement and tectonic significance for the Mesozoic-Recent evolution of northern Chile, paper presented at 6. Congreso Geológico Chileno, Serv. Nac. Geol. Miner., Viña del Mar, Chile 1991.
- Chavez, W., Geological setting and the nature and distribution of disseminated copper mineralization of the Mantos district, Antofagasta Province, Chile.- Ph.D. thesis, 142 pp., Calif. Univ., Berkeley, 1985.
- Coira, B., J. Davidson, C. Mpodozis, and V. Ramos, Tectonic and magmatic evolution of the Andes of northern Argentina and Chile, *Earth Sci. Rev.*, **18**, 303-332, 1982.
- Dallmeyer, R.D., M. Brown, J. Grocott, G.K. Taylor, and P.J. Treloar, Mesozoic magmatic and tectonic events within the Andean plate boundary zone, 26°-27°30'S, North Chile: Constraints from ⁴⁰Ar/³⁹Ar mineral ages, *J. Geol.*, **104**, 19-40, 1996.
- Damm, K.W., S. Pichowiak, and W. Todt, Geochemie, Petrologie und Geo-chronologie der Plutonite und des metamorphen Grundgebirges in Nordchile, *Berl. Geowiss. Abh., Reihe A*, **66**, 73-146, 1986.
- Delaney, P.T., D.D. Pollard, J.I. Ziony, and E.H. McKee, Field relations between dikes and joints: Emplacement processes and paleostress analysis, *J. Geophys. Res.*, **91**, 4920-4938, 1986.
- Diaz, M., U.G. Cordani, K. Kawashita, L. Baeza, R. Venegas, F. Herve, and F. Munizaga, Preliminary radiometric ages from the Mejillones Peninsula, northern Chile, *Comun., Santiago*, **35**, 59-67, 1985.
- Emeryman, S.H., and R. Marrett, Why dikes?, *Geology*, **18**, 231-233, 1990.
- Fitch, T.J., Plate convergence, transcurrent faults, and internal deformation adjacent to Southeast Asia and western Pacific, *J. Geophys. Res.*, **77**, 4432-4460, 1972.
- Forsythe, R., and L. Chisholm, Paleomagnetic and structural constraints on rotation in the north Chilean Coast Ranges, *J. S. Am. Earth Sci.*, **7**, 279-294, 1994.
- Furukawa, Y., Depth of the decoupling plate interface and the thermal structure under arcs, *J. Geophys. Res.*, **98**, 20,005-20,013, 1993a.
- Furukawa, Y., Magmatic processes under arcs and formation of the volcanic front, *J. Geophys. Res.*, **98**, 8309-8319, 1993b.
- García, F., Geología del Norte Grande de Chile, in *Seminario sobre el Geosinclinal Andino*, Empresa Nacional de Petróleo, Santiago, Chile, 1967.
- Geist, E.L., and D.W. Scholl, Application of continuum models to deformation of the Aleutian island arc, *J. Geophys. Res.*, **97**, 4953-4967, 1992.
- Gephart, J.W., Nazca - South America Plate interactions and uplift of the central Andean plateau (abstract), *EOS Trans. AGU*, **75** (45), Fall Meet. Suppl., F609, 1994.
- González, G., Evolución tectónica de la Cordillera de la Costa de Antofagasta (Chile): Con especial referencia a las deformaciones sinmagmáticas del Jurásico-Cretácico Inferior, *Berl. Geowiss. Abh., Reihe A*, **181**, 1-111, 1996.
- Gradstein, F.M., F.P. Agterberg, J.G. Ogg, J. Hardenbol, P. van Veen, J. Thierry and Z. Huang, A Mesozoic time scale, *J. Geophys. Res.*, **99**, 24,051-24,074, 1994.
- Grocott, J., M. Brown, R.D. Dallmeyer, G.K. Taylor, and P.J. Treloar, Mechanisms of continental growth in extensional arcs: An example from the Andean plate-boundary zone, *Geology*, **22**, 391-394, 1994.
- Hervé, M., Movimiento sinistral en el Cretácico Inferior de la Zona de Falla Atacama al Norte de Paposo (24°S) Chile, *Rev. Geol. de Chile*, **No. 31**, 37-42, 1987.
- Hervé, M., and N. Marinovic, Geocronología y evolución del batolito Vicuña Mackena, Cordillera de la Costa, Sur de Antofagasta (24-25°S), *Rev. Geol. de Chile*, **Vol. 16**, 31-49, 1989.
- Hollister, L.S., and M.L. Crawford, Melt-enhanced deformation: A major tectonic process, *Geology*, **14**, 558-561, 1986.
- Jaillard, E., P. Soler, G. Carlier, and T. Mourier, Geodynamic evolution of the northern and central Andes during early to middle Mesozoic times: A Tethyan model, *J. Geol. Soc. London*, **147**, 1009-1022, 1990.
- Jarrard, R.D., Relations among subduction parameters, *Rev. Geophys.*, **24**, 217-284, 1986.
- Kossler, A., Bajocian (Middle Jurassic) volcano-sedimentary sequences in the Coastal Cordillera of northern Chile, *Zentralbl. Geol. Paläont.*, **1**, Vol. 1996, 845-851, 1996.
- Krohe, A., Emplacement of synkinematic plutons in the Variscan Odenwald (Germany) controlled by transtensional tectonics, *Geol. Rundsch.*, **80**, 391-409, 1991.
- Larson, R.L., and W.C. Pitman III, World-wide correlation of Mesozoic magnetic anomalies, and its implications, *Geol. Soc. Am. Bull.*, **83**, 3645-3662, 1972.
- Liu, X., K.C. McNally, and Z.-K. Shen, Evidence for a role of the downgoing slab in earthquake slip partitioning at oblique subduction zones, *J. Geophys. Res.*, **100**, 15,351-15,372, 1995.
- Lucassen, F., and G. Franz, Arc-related Jurassic igneous and metaigneous rocks in the Coastal Cordillera of northern Chile/Region Antofagasta, *Lithos*, **32**, 273-298, 1994.
- Lucassen, F., and G. Franz, Magmatic arc metamorphism: Petrology and temperature history of metabasic rocks in the Coastal Cordillera of northern Chile, *J. Metamorph. Geol.*, **14**, 249-265, 1996.
- Makshev, V., Metallogeny, geological evolution, and thermochronology of the Chilean Andes between latitudes 21° and 26° South, and the origin of major porphyry copper deposits, Ph.D. thesis, 554 pp., Dalhousie Univ., Halifax, N.S., Canada, 1990.
- Marinovic, S., I. Smoje, V. Makshev, M. Hervé, and C. Mpodozis, Hoja Aguas Blancas, *Carta Geológica de Chile No. 70*, Serv. Nac. Geol. Miner., Santiago, 1995.
- Marrett, R., and R.W. Allmendinger, Estimates of strain due to brittle faulting: Sampling of fault populations, *J. Struct. Geol.*, **13**, 735-738, 1991.
- Miura, S., H. Ishii, and A. Takagi, Migration of vertical deformations and coupling of island arc plate and subducting plate, in *Slow Deformation and Transmission of Stress in the Earth*, *Geophys. Monogr. Ser.*, vol. 49, edited by S.C. Cohen and P. Vanicek, pp. 125-138, AGU, Washington, D.C., 1989.
- Müller, R.D., W.R. Roest, J.-Y. Royer, L.M. Gahagan, and J.G. Sclater, Digital isochrons of the world's ocean floor, *J. Geophys. Res.*, **102**, 3211-3214, 1997.
- Peacock, S.M., Blueschist-facies metamorphism, shear heating, and P-T-t paths in subduction zones, *J. Geophys. Res.*, **97**, 17,693-17,707, 1992.
- Platt, J.P., Mechanics of oblique convergence, *J. Geophys. Res.*, **98**, 16,239-16,256, 1993.
- Ponko, S.C., and S.M. Peacock, Thermal modeling of the southern Alaska subduction zone: Insight into the petrology of the subducting slab and overlying mantle wedge, *J. Geophys. Res.*, **100**, 22,117-22,128, 1995.
- Price, N.J., and J.W. Cosgrove, *Analysis of Geological Structures*, 502 pp., Cambridge Univ. Press, New York, 1990.

- Prinz, P., H.G. Wilke, and A. von Hillebrandt, Sediment accumulation and subsidence history in the Mesozoic marginal sea in N-Chile, in *Tectonics of the Southern Central Andes*, edited by K.-J. Reutter, E. Scheuber, and P. Wigger, pp. 219-233, Springer-Verlag, New York, 1994.
- Randall, D.E., G.K. Taylor, and J. Grocott, Major crustal rotations in the Andean margin: Paleomagnetic results from the Coastal Cordillera of northern Chile, *J. Geophys. Res.*, **101**, 15,783-15,798, 1996.
- Reutter, K.J., E. Scheuber, and G. Chong, The Pre-cordilleran fault system of Chuquicamata, Northern Chile: Evidence for reversals along arc-parallel strike-slip faults, *Tectonophysics*, **259**, 213-228, 1996.
- Riley, P.D., M.E. Beck, and R.F. Burmester, Paleomagnetic evidence of vertical block rotations from the Mesozoic of northern Chile, *J. Geophys. Res.*, **98**, 8321-8333, 1993.
- Rogers, G., and C.J. Hawkesworth, A geochemical traverse across the north Chilean Andes: evidence for crust generation from the mantle wedge, *Earth Planet. Sci. Lett.*, **91**, 271-285, 1989.
- Roperch, P., and G. Carlier, Paleomagnetism of Mesozoic rocks from the central Andes of southern Peru: Importance of rotations in the development of the Bolivian Orocline, *J. Geophys. Res.*, **97**, 17,233-17,249, 1992.
- Roperch, P., G. Dupont-Nivet, and L. Pinto, Rotaciones tectónicas en el Norte de Chile, paper presented at *VIII Congreso Geológica Chileno*, Universidad Católica del Norte, Antofagasta, Chile, 1997.
- Rössling, R., Petrologie in einem tiefen Stockwerk des jurassischen magmatischen Bogens in der nordchilenischen Küstenkordillere südlich von Antofagasta, *Berl. Geowiss. Abh., Reihe A*, **112**, 1-73, 1989.
- Royden, L.H., The steady state thermal structure of eroding orogenic belts and accretionary prisms, *J. Geophys. Res.*, **98**, 4487-4507, 1993.
- Scheuber, E., Tektonische Entwicklung des nordchilenischen aktiven Kontinentalrandes: Der Einfluß von Plattenkonvergenz und Rheologie, *Geotekton. Forsch.*, **81**, 1-131, 1994.
- Scheuber, E., and P.A.M. Andriessen, The kinematic and geodynamic significance of the Atacama Fault Zone, northern Chile, *J. Struct. Geol.*, **12**, 243-257, 1990.
- Scheuber, E., and K.-J. Reutter, Magmatic arc tectonics in the central Andes between 21° and 25° S, *Tectonophysics*, **205**, 127-140, 1992.
- Scheuber, E., K. Hammerschmidt, and H. Friedrichsen, ⁴⁰Ar/³⁹Ar and Rb-Sr analyses from ductile shear zones from the Atacama Fault Zone, northern Chile: the age of deformation, *Tectonophysics*, **250**, 61-87, 1995.
- Schmidt, M.W., Amphibole composition in tonalite as a function of pressure: An experimental calibration of the Al-in-hornblende barometer, *Contrib. Mineral. Petrol.*, **110**, 304-310, 1992.
- Shimamoto, T., The origin of S-C mylonites and a new fault-zone model, *J. Struct. Geol.*, **11**, 51-64, 1989.
- Skarmeta, J., Análisis estructural de diques deformados en la Península de Mejillones, Norte de Chile, *Rev. Geol. Chile*, **9**, 3-16, 1980.
- Sperner, B., L. Ratschbacher, and R. Ott, Fault-surface analysis: A turbo pascal program package for graphical representation and reduced stress tensor calculation, *Comput. Geosci.*, **19**, 1361-1388, 1993.
- Thomas, A.L., and D.D. Pollard, The geometry of echelon fractures in rock: Implications from laboratory and numerical experiments, *J. Struct. Geol.*, **15**, 323-334, 1993.
- Tichelaar, B.W., and L.J. Ruff, Depth of seismic coupling along subduction zones, *J. Geophys. Res.*, **98**, 2017-2037, 1993.
- Uyeda, S., and H. Kanamori, Back-arc opening and the mode of subduction, *J. Geophys. Res.*, **84**, 1049-1061, 1979.
- Wallbrecher, E., and W. Unzog, Gefüge 6, ein Programm-Paket zur Auswertung von Richtungsdaten, University of Graz, Graz, Austria, 1997.
- Wang, K., T. Mulder, G.C. Rogers, and R.D. Hyndman, Case for very low coupling stress on the Cascadia subduction fault, *J. Geophys. Res.*, **100**, 12,907-12,918, 1995.
- Wdowinski, S., and Y. Bock, The evolution of deformation and topography of high elevated plateaus, 2, Application to the central Andes, *J. Geophys. Res.*, **99**, 7121-7130, 1994.
- Woodcock, N.H., The role of strike-slip fault systems at plate boundaries, *Philos. Trans. R. Soc. London, Ser. A*, **317**, 13-29, 1986.
- Zoback, M.L., First- and second-order patterns of stress in the lithosphere: The world stress map project, *J. Geophys. Res.*, **97**, 11,703-11,728, 1992.
- Zonenshayn, L.P., L.A. Savostin, and A.P. Sedov, Global paleogeodynamic reconstructions for the last 160 million years, *Geotectonics*, **18**, 181-195, 1984.

G. Gonzalez, Departamento de Ciencias Geológicas, Universidad Católica del Norte, Casilla 1280, Antofagasta, Chile (ggonzalc@socompa.ucn.cl)
 E. Scheuber, Institut für Geologie, Geophysik und Geoinformatik, Freie Universität Berlin, Maltesserstrasse 74-100, Berlin, Germany. (scheuber@geophysik.fu-berlin.de)

(Received November 15, 1996;
 revised November 9, 1998;
 accepted May 10, 1999.)